

# HIGH ACCURACY DIFFERENTIAL AND KINEMATIC GPS POSITIONING USING A DIGITAL BEAM-STEERING RECEIVER

Dan Sullivan, Randy Silva and Alison Brown NAVSYS Corporation

## ABSTRACT

The time, orbit and attitude data, obtained from GPS, enables spacecraft system developers to accomplish autonomous orbit maneuver planning and autonomous stationkeeping maneuvers on-board the spacecraft. Current generation GPS navigation will provide accuracy on the order of 2 to 5 meters. For future missions, which will involve formation flying of clusters of small satellites, more precise relative positioning accuracy is required. This can be achieved through the use of differential GPS (DGPS) and kinematic GPS (KGPS) relative positioning techniques. These techniques remove the effect of common GPS system errors between the cluster of satellites, leaving only the effect of receiver measurement errors on the precise positioning solution.

## INTRODUCTION

Using next generation GPS digital beam-steering technology, the GPS measurement accuracy can be significantly improved through the use of digital beam steering to increase the gain in the direction of the GPS satellites. This improves the measurement accuracy by reducing the measurement noise and also reduces the effect of multipath on the pseudo-range and carrier-phase observations. The improved measurement accuracy results in better precision for DGPS and KGPS corrections and also faster convergence for kinematic cycle ambiguity resolution.

In this paper, the principles of DGPS and KGPS relative positioning are described and test results are presented showing the performance advantages of

digital beam-forming for precise DGPS positioning, for performing rapid ambiguity resolution for KGPS positioning, and in reducing the effect of multipath errors on both code and carrier observations.

## KINEMATIC POSITIONING ALGORITHM

The steps followed by the relative kinematic positioning algorithm developed by NAVSYS are illustrated in Figure 1. Kinematic positioning and alignment relies on the relationship of the carrier phase observations to the range observations described in the following equation.

### Equation 1

$$PR_1 = R + bu_1 + b_{SVPR1} + T + I_1 + n_{PR1}$$

$$PR_2 = R + bu_2 + b_{SVPR2} + T + I_1 \frac{\lambda_2^2}{\lambda_1^2} + n_{PR2}$$

$$-CPH_1 = R + bu_{CPH1} + b_{SVCPH1} + T - I_1 + n_{CPH1} - N_1 \lambda_1$$

$$-CPH_2 = R + bu_{CPH2} + b_{SVCPH2} + T - I_1 \frac{\lambda_2^2}{\lambda_1^2} + n_{CPH2} - N_2 \lambda_2$$

where

PR = pseudo-range on L1 or L2 frequencies (meters)

CPH = carrier phase on L1 or L2 frequencies (meters)

$R_T$  = true range (meters)

bu = range equivalent receiver clock offset (meters)

bsv = range equivalent satellite clock offset (meters)

T = tropospheric delay (meters)

I = ionospheric delay (meters)

n = measurement noise (meters)

N = CPH integer (cycles)

$\lambda$  = carrier wavelength (meters)

The pseudo-range observations observe the range from the GPS satellites to the UE (R) offset by the user and satellite clock (b), the tropospheric delay (T) and the ionospheric delay (I). The ionospheric delay is different on the L1 and L2 observations as it is inversely proportional to the frequency squared and so can be removed from the PR by differencing. The DGPS corrections will remove any errors in the navigation solution caused by satellite position and clock offsets. The accuracy of the PR derived DGPS corrected position solution is a function of the pseudo-range noise, which includes receiver noise and multipath errors. The GPS/inertial navigation solution will filter the short-term noise effects, but it cannot correct for correlated noise errors from multipath. This results in the final DGPS corrected solution accuracy and are generally on the order of 1 to 1.5 meters due to these uncorrected errors.

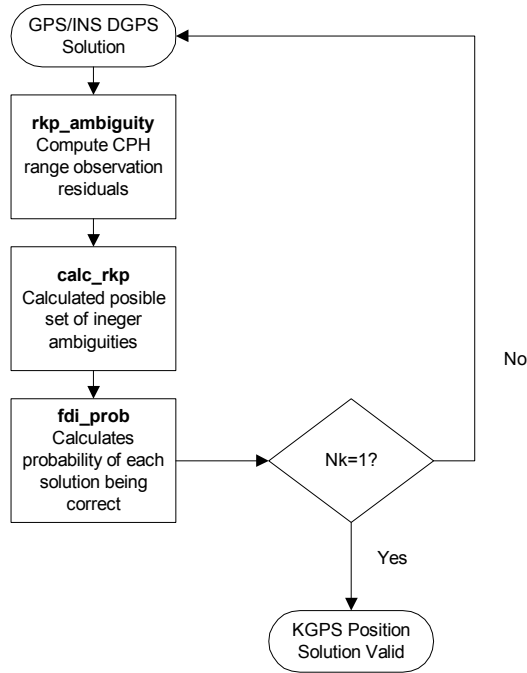


**Figure 1 Kinematic Positioning Algorithm**

The effect of multipath is much smaller on the GPS carrier phase observations. As shown in Equation 1, the carrier phase (CPH) observation provides the same observability of user position through the range to the GPS satellite but includes an additional uncertainty of the integer number of cycles to the satellite (N). If this integer ambiguity is resolved, then the position accuracy derived from the CPH observation accuracy is a function of the carrier phase noise and carrier multipath errors which are on the order of a few centimeters. The process of

resolving this integer cycle ambiguity is generally termed cycle ambiguity resolution and is the key to performing kinematic GPS positioning.

The steps employed by the kinematic positioning algorithm to resolve the integer ambiguity are illustrated in Figure 1 and described below.

### rkp\_ambiguity

The first step is to create the carrier phase corrected measurement residuals. These are derived from the following equation and include: carrier phase corrections (CPC) from the reference location, estimated range to the satellite from the DGPS solution, and the estimated atmospheric errors (tropo and iono). As shown in the following equation, this measurement residual observes the position error in the DGPS solution (relative to the reference location), the residual ionospheric and tropospheric errors and the integer ambiguity offset. This reduces the ambiguity resolution process to a single (wide-lane) ambiguity  $N_W = N_1 - N_2$ . The wide-lane wavelength is 86 cm as opposed to the L1 wavelength of 19 cm. This larger resolution wavelength is easier to observe allowing ambiguity resolution to occur much faster with L1/L2 dual frequency observations than for single frequency (L1 only) GPS. To remove the effect of the clock bias, the single-differenced observations are used (zsd) since the clock bias is common between the GPS satellite observations

### Equation 2

$$\begin{aligned}
 z_{CPH1} &= -CPH_1 - \hat{R} - \hat{b}_{SVCPH1} + \hat{C}PC_1 - \Delta\hat{T} + \Delta\hat{I}_1 \\
 &= \mathbf{1}^T \tilde{\mathbf{x}} + bu_{CPH1} + (\tilde{T} - \tilde{I}_1) + n_{CPH1} - N_1 \lambda_1 \\
 z_{CPH2} &= -CPH_2 - \hat{R} - \hat{b}_{SVCPH2} + \hat{C}PC_2 - \Delta\hat{T} + \Delta\hat{I}_2 \\
 &= \mathbf{1}^T \tilde{\mathbf{x}} + bu_{CPH1} + (\tilde{T} - \tilde{I}_1 \frac{\lambda_2^2}{\lambda_1^2}) + n_{CPH2} - N_2 \lambda_2 \\
 z_{CPHW} &= \left( \frac{z_{CPH1}}{\lambda_1} - \frac{z_{CPH2}}{\lambda_2} \right) \lambda_W \\
 &= \mathbf{1}^T \tilde{\mathbf{x}} + bu_{CPH1} + \tilde{T} - \tilde{I}_1 \frac{\lambda_W}{\lambda_1} \left( 1 - \frac{\lambda_2}{\lambda_1} \right) \\
 &\quad + n_{CPH1} \frac{\lambda_W}{\lambda_1} - n_{CPH2} \frac{\lambda_W}{\lambda_2} - N_W \lambda_W \\
 \lambda_W^{-1} &= \lambda_1^{-1} - \lambda_2^{-1} \quad N_W = N_1 - N_2
 \end{aligned}$$

### calc\_rkp

The purpose of the calc\_rkp function is to compute the set of possible ambiguities for each of the satellite observations. This is performed by computing all of the likely ambiguities based on an initial search space that the ambiguity solution must fall within (see Figure 2). The search space is dictated by the initial uncertainty of the GPS/inertial navigation solution ( $P_{DGPS}$ ). Each ambiguity must pass the following criteria to be considered a valid member of the ambiguity set (Nset). The geometry vector H is calculated from the satellite line of sight vectors. The scale factor  $\alpha$  is computed based on the desired probability of missed detection for the KGPS solution, based on the equation below.

### Equation 3

$$\underline{NN}^T < \alpha H E[\tilde{x}\tilde{x}^T] H^T / \lambda_w^2 = \alpha H \frac{P_{DGPS}}{\lambda_w^2} H^T \quad \underline{N} \in Nset$$

$$P_{MD} = \chi^2(\alpha|3)$$

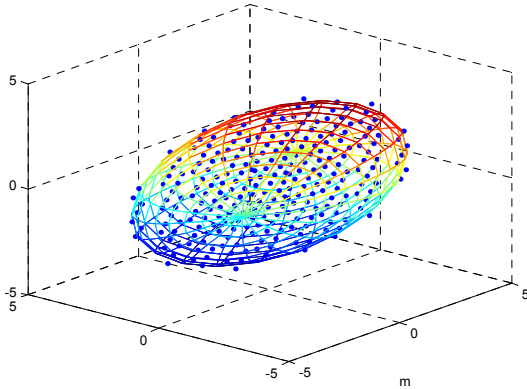


**Figure 2 GPS/Inertial Solution Space Ambiguity Set**

### fdi\_prob

The correct ambiguity from the set is isolated by using an integrity check to reject the incorrect solutions. For the correct ambiguity solution, the fault vector (f), computed from the following equation will include only the receiver noise errors. For all other values, the f vector will also include errors due to the ambiguity error.

### Equation 4

$$\underline{f} = S(N_w \lambda_w + \underline{z}_{CPHW})$$

$$= S \left( H \tilde{x} + \tilde{T} - \tilde{T}_1 \frac{\lambda_w}{\lambda_1} \left( 1 - \frac{\lambda_2}{\lambda_1} \right) + \underline{n}_{CPH1} \frac{\lambda_w}{\lambda_1} - \underline{n}_{CPH2} \frac{\lambda_w}{\lambda_2} \right) \approx \underline{n}$$

$$S = I - HH^* \quad SH = 0 \quad H^* = (H^T H)^{-1} H^T$$

The S matrix has Nsv-4 degrees of freedom. As the number of GPS satellites in the solution increases, the ability to distinguish between the different members of Nset improves, and also the initial DGPS search space ellipse gets smaller. The f vector is accumulated over multiple samples to determine the correct ambiguity. The smaller the noise (n) on the observation, the faster the algorithm can differentiate between the different ambiguities and pick the correct solution to allow kinematic positioning to be performed.

### Pseudo-Range and Carrier-Phase GPS Corrections

The pseudo-range and carrier-phase correction messages are generated using observations from a reference receiver. The pseudo-range corrections are used to compute the DGPS navigation solution. The carrier-phase corrections are used to compute the KGPS positioning solution. The messages generated include the following information. This format is in accordance with RTCM SC-104 [1].

### PRC Message (repeated for each of Nsvs on L1 and L2)

- Time                      GPS time of correction
- PRN                        SVID correction applies to
- PRC                        Pseudo-range correction (meters)
- RRC                        Rate of change of correction (m/s)
- IOD                        Issue of data for related ephemeris used
- Sigma\_prc                Estimated accuracy of correction (m)

### CPC Message (repeated for each of Nsvs on L1 and L2)

- Time                      GPS time of correction
- PRN                        SVID correction applies to
- CPC                        Carrier-phase correction (meters)
- DCPC                      Rate of change of correction (m/s)

- CLOC            Loss of phase lock counter (indicates ambiguity must be recomputed)
- Sigma\_cph      Estimated accuracy of correction (m)

**MULTIPATH ERRORS**

Multipath errors are caused by the receiver tracking a composite of the direct GPS signals and reflected GPS signals from nearby objects, such as the ground, or a building or ship’s mast (see Figure 3). Multipath errors can be observed by their effect on the measured signal/noise ratio and the code and carrier observations, as described below.<sup>[2,3,4]</sup>

Signal/Noise Ratio When multipath is present the signal/noise ratio magnitude varies due to the constructive and destructive interference effect. The peak-to-peak variation is an indication of the presence of multipath signals, as shown by the following equation where A is the amplitude of the direct signal, A<sub>M</sub> is the amplitude of the reflected multipath signal, θ is the carrier phase offset for the direct signal and θ<sub>M</sub> is the carrier phase offset for the multipath signal.

$$\tilde{A} = |A + A_M e^{j\Delta\theta}| - A$$

$$\tilde{\theta} = \angle(A + A_M e^{j\Delta\theta})$$

$$\Delta\theta = \theta - \theta_M$$

The multipath carrier phase error ( $\tilde{\theta}$ ) is related to the received multipath power level from the above equation. This results in a cyclic carrier phase error as the multipath signals change from constructive to destructive interference that has the peak-to-peak carrier phase error shown in Figure 5. Multipath also causes the signal-to-noise ratio to vary between the peak and minimum levels shown in Figure 4 depending on the relative Multipath/Signal (M/S) strength. For low elevation GPS satellite signals, it is quite common to get M/S received power levels as high as -3 dB. This will cause a cyclic error on the carrier phase observations of around +/- 2 cm. For precision Kinematic Carrier Phase Tracking (KCPT) GPS applications, this error will affect the ability to perform rapid carrier cycle ambiguity resolution<sup>5</sup>. In this paper, preliminary test results are included that show the performance advantages of a digital beam-steering receiver for minimizing multipath effects and providing precision kinematic GPS positioning.

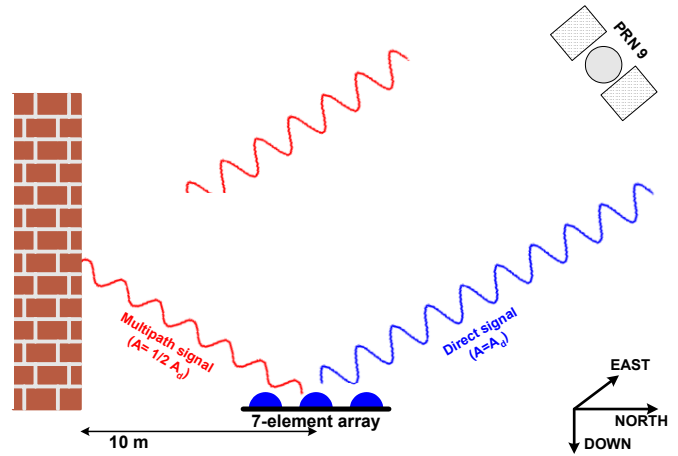


**Figure 3 Typical Multipath Scenario**

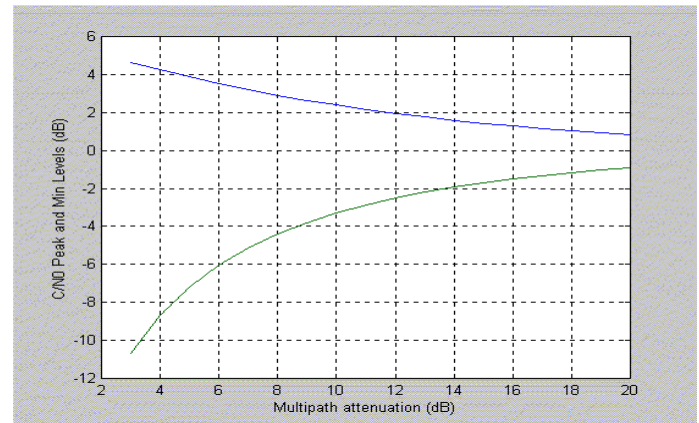


**Figure 4 Multipath Amplitude Effect**

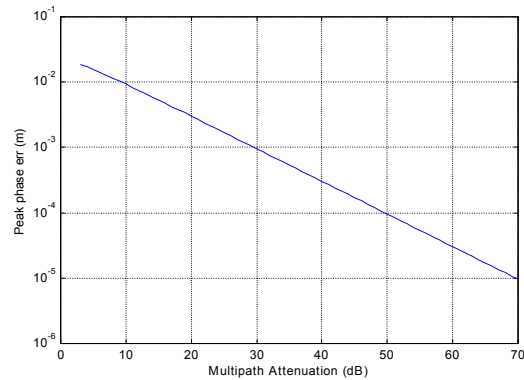


**Figure 5 Multipath Peak Phase error vs. Attenuation (dB)**

**HAGR PRINCIPLE OF OPERATION**

The NAVSYS High-gain Advanced GPS Receiver (HAGR) is a digital beam steering receiver designed for GPS satellite radio navigation and other spread spectrum applications. This is available for both

military and commercial precision GPS applications and uses the modular assembly shown in Figure 6 to allow it to be easily configured to meet a user's specific requirements. A space-based HAGR configuration is currently being developed by NAVSYS under contract to AFRL/VS and NASA GSFC<sup>6</sup>.



**Figure 6 HAGR Assembly**

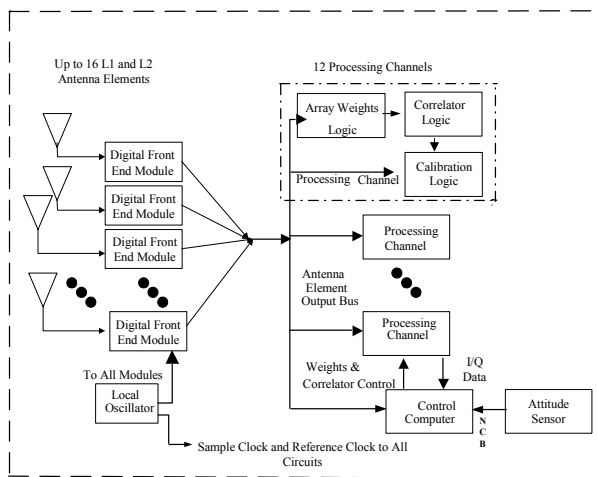


**Figure 7 HAGR System Architecture**

The HAGR system architecture is shown in Figure 2. The signal from each antenna element is first digitized using a Digital Front-End (DFE). This bank of digital signals is then used to create the composite digital beam-steered signal input for each of the receiver channels by applying a complex weight to combine the antenna array outputs. As

shown in Figure 2, the array weights are applied independently for each of the satellite channels. This allows the antenna array pattern to be optimized for each satellite signal tracked.

The weights for each channel are dynamically downloaded through software control. The HAGR software can automatically calculate the beam steering pattern for each satellite based on the known receiver location, the broadcast GPS satellite location and the input attitude of the antenna array. For static applications, the array can either be configured pointing north (the default attitude) or the actual attitude is programmed into the configuration file. For mobile applications, the antenna array attitude is input through a serial port from either a magnetic compass and tilt sensor or an inertial navigation system. The HAGR also includes a mode where the antenna weights are read from a user definable file based on the satellite azimuth and elevation. Matlab tools exist for creating these antenna weights based on specific user requirements.

In Figure 8 and Figure 9, the antenna patterns created by the digital antenna array are shown for four of the satellites tracked. The HAGR can track up to 12 satellites simultaneously. The antenna pattern provides the peak in the direction of the satellite tracked (marked 'x' in each figure). The beams follow the satellites as they move across the sky. Since the L2 wavelength is larger than the L1 wavelength, the antenna beam width is wider for the L2 antenna pattern than for the L1.

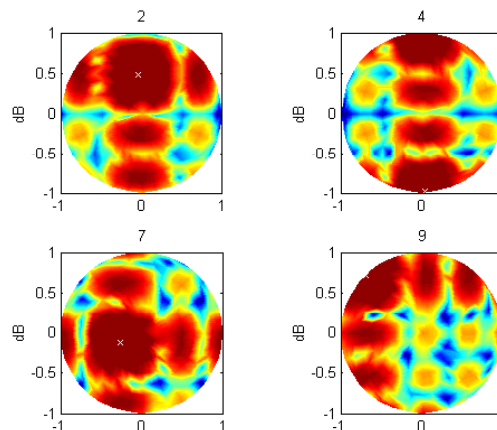


**Figure 8 L1 Antenna Pattern**

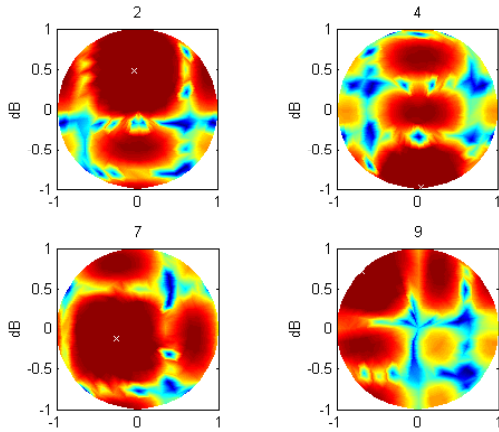


Figure 9 L2 Antenna Pattern

### MULTIPATH MINIMIZATION TESTING

To evaluate the multipath performance improvements, testing was performed by partitioning the HAGR 7-element antenna array (see Figure 10) into two 4-element sub-arrays, as shown in Figure 11. The carrier phase errors provided by the individual antenna elements and the digital beam-steered results from the two sub-arrays was compared. When a full 7-element HAGR array is used, further performance improvements could be expected over the dual 4-element test results presented here. To quantify the level of multipath, both the carrier phase relative to the center element and the signal amplitude is plotted in Figure 12 and Figure 13. From the peak-to-peak variation of the IQ amplitude,  $A_{pp} \approx 40$ , and phase,  $\Delta\theta \approx 2cm$ , we can see that the signal to multipath ratio is roughly 5 dB using a single element (see Figure 4 and Figure 5).



Figure 10 HAGR 7-Element Array

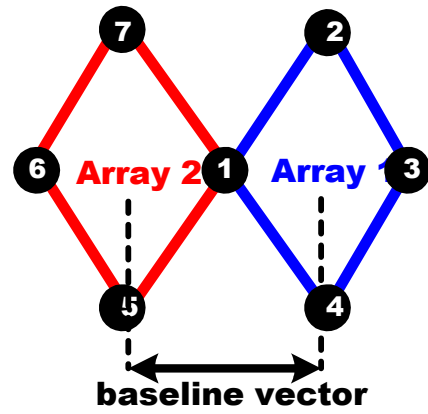


Figure 11 HAGR Dual Sub-array Test Setup

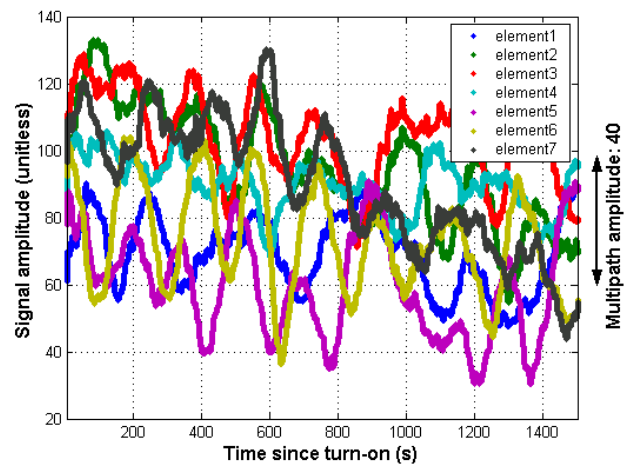


Figure 12 Amplitudes of array 1 elements (5s moving average)

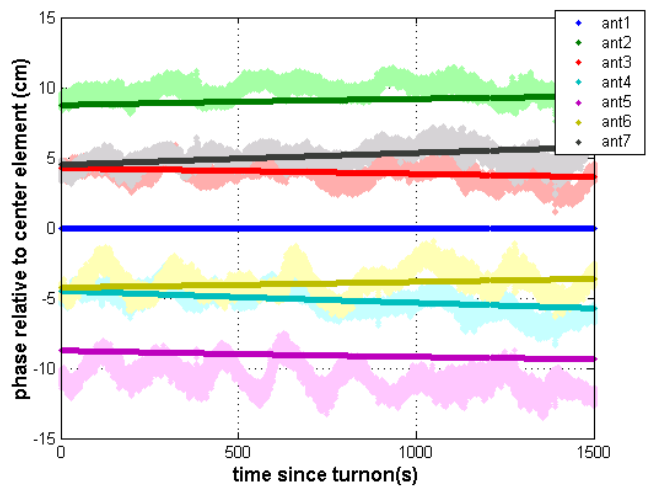
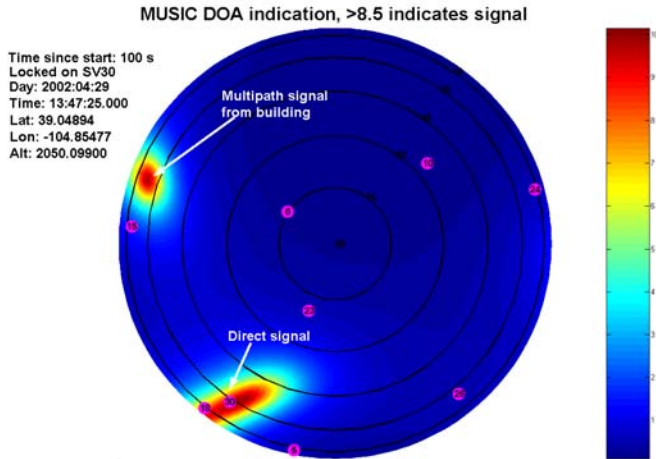


Figure 13 Carrier Phase of array 1 (thick lines: expected phase offset)

The spatial information from the 7-element phased array was also processed to identify the source of the multipath through direction of arrival (DOA) estimation using the MUSIC algorithm. The results shown in Figure 14 shows both the direct signals and a strong multipath signal being receiver from the NAVSYS' building.



**Figure 14 MUSIC direction of arrival estimation**

To test the single element and the digital beam-steered carrier phase accuracy, the carrier phase errors were compared between the center element and the two 4-element sub-arrays. These results are plotted in Figure 15 for both the single element and the beam-steered results. From this figure, the peak-to-peak phase error is in the order of 3.5 cm when using a single antenna element. With digital beamforming the phase error is reduced to about 1 cm.

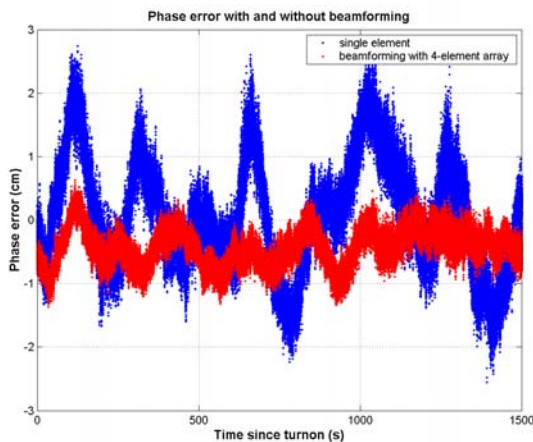


**Figure 15 Single Element and Digital Beam-Steered Carrier Phase Errors**

## HAGR KINEMATIC POSITIONING TEST DATA

To demonstrate the precise positioning performance possible when using the HAGR for kinematic positioning, a test was performed using the HAGR receiver located at NAVSYS facilities and the Alternate Master Clock (AMC2) reference station operating at Schriever AFB some 25 miles distant. The results from this kinematic positioning solution are shown in Figure 16 and Figure 17. The RMS position variation is between 2 to 9 cm on each axis (see Figure 17).

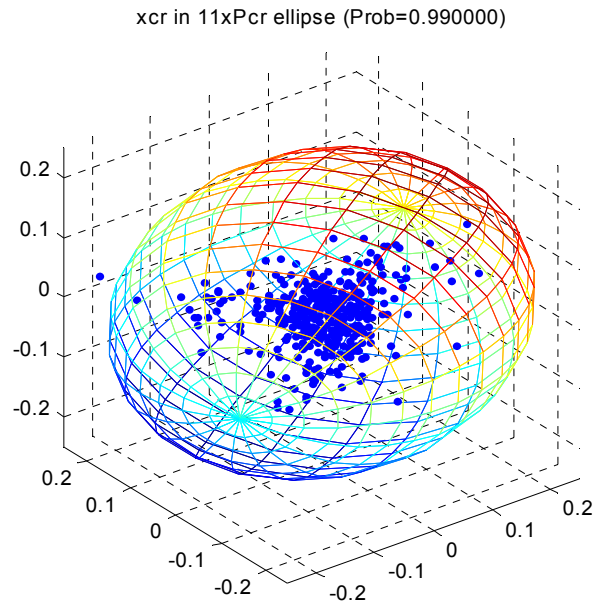


**Figure 16 HAGR Wideline Kinematic Position (relative to AMC2)**

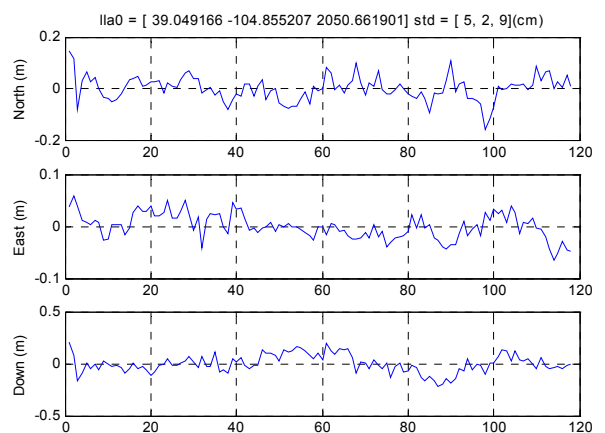


**Figure 17 NED Wideline Position Variation (m)**

The KGPS algorithm also estimates the carrier phase noise from the fault vector. From Figure 18 this

converges to a value of within 1 cm (0.04 cycles) for the L1 and L2 phase measurements. This phase noise includes both the effect of the HAGR carrier phase errors and also the AMC2 carrier phase errors. Further testing is planned at a later date to evaluate the performance improvements that could be achieved using a HAGR receiver as both the reference station and the remote unit for kinematic positioning

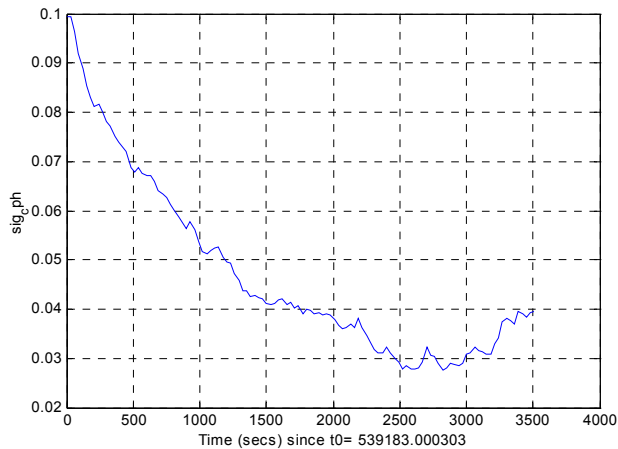


**Figure 18 Estimated Carrier Phase Noise from Fault Vector (cycles)**

## CONCLUSION

The testing performed to date has shown that there is a significant reduction in the peak-to-peak carrier phase error from multipath when using a digital beamsteering receiver. With dual 4-element sub-arrays, the peak-to-peak carrier phase error attributed to multipath was less than 1 cm compared to 3.5 cm when using a single antenna element. With a larger antenna array, the performance could be expected to further improve. The HAGR kinematic GPS position solution when operating with the AMC2 reference station located at Schriever AFB was within 2 – 9 cm (RMS) on each axis. This performance includes the carrier phase errors from both the HAGR and the AMC2 reference station.

Further testing is planned at a later date to show what further performance improvements could be achieved when using a HAGR as both a reference station and a remote receiver. The digital beamsteering capability will have significant advantages for precision space applications employing kinematic techniques, such as formation flying of clusters of satellites or automated rendezvous and

docking. The ability to provide precise carrier phase observations in the challenging space environment and minimize multipath errors from sources such as solar panels or arrays will allow rapid, robust ambiguity resolution to be performed even in this challenging space environment.

## ACKNOWLEDGEMENT

The kinematic test data in this paper was collected using a L1/L2 HAGR receiver purchased by the US Naval Observatory. The multipath testing was sponsored by NAVAIR for the SRGPS program. The authors would like to express their appreciation for this support.

## BIOGRAPHIES

Alison Brown is the President and CEO of NAVSYS Corporation. She has a PhD in Mechanics, Aerospace, and Nuclear Engineering from UCLA, an MS in Aeronautics and Astronautics from MIT, and an MA in Engineering from Cambridge University. In 1986, she founded NAVSYS Corporation. Currently she is a member of the Scientific Advisory Board for the USAF, a member of the Interagency GPS Executive Board Independent Advisory Team, and serves on the GPS World editorial advisory board.

Dan Sullivan is a Senior Scientist at NAVSYS Corporation. He is responsible for GPS/INS Integration mission area algorithms, architecture and software. Previously he was employed as a Senior Staff Engineer with Lockheed Martin Missiles and Fire Control in Orlando, Florida, where he was responsible for systems analysis and design for image-processing, target state estimation and sensor fusion for a variety of missile, fixed-wing and rotary-wing targeting systems. He has a MS in Electrical Engineering from Columbia University.

Randy Silva is a Senior Scientist at NAVSYS Corporation where his work includes simulation, design, implementation, and testing of real-time GPS/Inertial systems. He holds a B.A. in Computer Science from the University of Colorado.

## REFERENCES

- 1 RTCM Recommended Standards for Differential GNSS (Global Navigation Satellite Systems Service), RTCM SC-104, Version 2., January 3, 1994

- 2 A. Brown, "Performance and Jamming Test Results of a Digital Beamforming GPS Receiver," Proceedings of Joint Conference on Navigation, Orlando, Florida, May, 2002.
- 3 A. Brown, N. Gerein, "Test Results from Digital P(Y) Code Beamsteering Receiver for Multipath Minimization," ION 57th Annual Meeting, Albuquerque, New Mexico, September 2001.
- 4 A. Brown, "High Accuracy GPS Performance using a Digital Adaptive Antenna Array," Proceedings of ION National Technical Meeting 2001, Long Beach, CA, January 2001
- 5 A. Brown, K. Stolk, "Rapid Ambiguity Resolution using Multipath Spatial Processing for High Accuracy Carrier Phase, Proceedings of ION GPS 2002, Portland, OR, September 2002.
- 6 R. Silva, R. Worrell, and A. Brown, "Reprogrammable, Digital Beamsteering GPS Receiver Technology for Enhanced Space Vehicle Operations," Proceedings of 2002 Core Technologies for Space Systems Conference, Colorado Springs, CO, November 2002.